Published in final edited form as:
Radiother Oncol. 2013 January ; 106(1): 124–129. doi:10.1016/j.radonc.2012.09.003.

Proton therapy radiation pneumonitis local dose–response in esophagus cancer patients

Alfredo E. Echeverria[a,c], **Matthew McCurdy**[a,c], **Richard Castillo**[a], **Vincent Bernard**[b], **Natalia Velez Ramos**[b], **William Buckley**[a], **Edward Castillo**[a], **Ping Liu**[a], **Josue Martinez**[a], and **Thomas Guerrero**[a,*]

[a]The University of Texas M.D. Anderson Cancer Center, Houston

[b]The University of Puerto Rico, San Juan

[c]Baylor College of Medicine, Houston, USA

Abstract

Purpose—This study quantifies pulmonary radiation toxicity in patients who received proton therapy for esophagus cancer.

Materials/methods—We retrospectively studied 100 esophagus cancer patients treated with proton therapy. The linearity of the enhanced FDG uptake vs. proton dose was evaluated using the Akaike Information Criterion (AIC). Pneumonitis symptoms (RP) were assessed using the Common Toxicity Criteria for Adverse Events version 4.0 (CTCAEv4). The interaction of the imaging response with dosimetric parameters and symptoms was evaluated.

Results—The RP scores were: 0 grade 4/5, 7 grade 3, 20 grade 2, 37 grade 1, and 36 grade 0. Each dosimetric parameter was significantly higher for the symptomatic group. The AIC winning models were 30 linear, 52 linear quadratic, and 18 linear logarithmic. There was no significant difference in the linear coefficient between models. The slope of the FDG vs. proton dose response was 0.022 for the symptomatic and 0.012 for the asymptomatic ($p = 0.014$). Combining dosimetric parameters with the slope did not improve the sensitivity or accuracy in identifying symptomatic cases.

Conclusions—The proton radiation dose response on FDG PET/CT imaging exhibited a predominantly linear dose response on modeling. Symptomatic patients had a higher dose response slope.

Keywords

Radiation pneumonitis; Proton therapy; Positron emission tomography

Thoracic radiotherapy injures portions of the lung that are not involved with cancer [1-5]. Proton therapy has been proposed as a modality with the potential to reduced normal tissue toxicity. This potential benefit of proton therapy comes from the Bragg peak, which allows the maximal dose to be concentrated to the target region with minimal exposure beyond [6]. This should allow for the development of radiation plans with an improved therapeutic

*Corresponding author. Address: Department of Radiation Oncology – Unit 97, The University of Texas M.D. Anderson Cancer Center, 1515 Holcombe Blvd., Houston, TX 77030, USA. tguerrero@mdanderson.org (T. Guerrero).

Conflicts of interest statement
The authors have no commercial or financial interests related to this study to disclose.

index, an increased tumoricidal effect while reducing normal tissue toxicity [7,8]. Several studies have reported improvements of local control and disease-free survival with the use of proton therapy [9,10]. However, proton therapy involves several physical and technical uncertainties, including uncertainties regarding the damage it may cause to normal tissues [7,11-16]. Most toxicity reports in the literature rely on subjective toxicity assessment and correlations with parameters extracted from the treatment plans [17-20]. To date, there has not been an objective measurement of the normal human lung proton therapy dose response.

Radiation pneumonitis (RP) is the most severe complication that occurs following thoracic radiotherapy and is potentially fatal [21]. RP is an inflammatory reaction that takes place within lung tissue in response to radiation damage [22-24]. Pulmonary inflammatory processes can be imaged using [^{18}F]-fluorodeoxyglucose positron emission tomography (FDG PET) [25,26]. We previously utilized restaging FDG PET/Computed Tomography (FDG PET/CT) images to provide an objective and quantitative measurement of the radiation dose response of the lungs after thoracic X-ray radiotherapy [27-29]. We observed a linear relationship between the radiation dose and FDG pulmonary uptake for each individual [27]. We call the slope of this dose response the pulmonary metabolic radiation dose response (PMRR). We also found a statistically significant correlation between PMRR and RP clinical symptoms [28,29]. We used the PMMR to demonstrate an increased RP toxicity associated with the degree of taxane use [29].

Population studies of RP found dosimetric parameters, such as the mean lung dose (MLD), associate with the risk to develop symptomatic RP [30-32]. Methods to individualize the risk assessment by adjusting the probability of RP based on the odds ratio associated with the presence of dose-independent risk factors have been proposed [33]. However, the individual pulmonary RP dose–response for proton therapy is unknown. In a toxicity modeling study, Seppenwoolde et al. [35] found a linear local-dose response best explained the incidence of RP on the basis of the individual dose distributions. Knowledge of the individual RP dose–response would guide treatment strategies, such as, whether a little dose to a large amount of lung or a high dose to small amount of lung is more critical for induction of RP [34]. Patients with esophageal cancer routinely undergo restaging FDG PET/CT 6 weeks after neoadjuvant chemoradiation therapy to identify interval metastases. Using the restaging FDG PET/CT imaging as a surrogate for the local dose RP response we found the local-dose response of the lungs is indeed linear for X-ray therapy [27].

In this retrospective study, the local pulmonary dose response relationship is evaluated on post-treatment FDG PET imaging in esophagus cancer patients who received proton therapy. We hypothesize the individual RP dose–response for proton radiation is linear with symptomatic patients possessing a more intense response.

Materials and methods

The study population comprised patients treated at the University of Texas M.D. Anderson Proton Therapy Center for esophagus cancer between July 12, 2006 and April 1, 2011 (n = 100) who had restaging PET/CT imaging between 21 and 86 days after completion of proton therapy. Proton beam treatment planning was performed using the Eclipse treatment planning system (Varian Medical Systems, Palo Alto, CA) and the radiation dose was calculated using the average CT obtained from 4D CT image sets. All proton therapy treatment plans were prospectively reviewed for quality assurance by 10 radiation oncologists who specialize in thoracic malignancies. Patient identifiers were removed in accordance with a retrospective study protocol (PA11-0801) approved by the M.D. Anderson Institutional Review Board.

Study subjects had FDG PET/CT images between 21 and 86 days after completion of radiotherapy for interval restaging evaluation [37]. Image analysis was performed using custom Matlab software (v2011a, Mathworks, Inc.). Lung segmentation was applied to the treatment planning CT and the restaging PET/CT images using Hounsfield units between −920 and −250 plus connectivity. Residual trachea, main stem bronchial, and second division bronchi were removed manually. The resulting binary lung regions of interest (lung ROI) were used in subsequent analyses. Mean lung dose (MLD), the volume of lung irradiated to 5, 10 and 20 CGE (V_5, V_{10}, V_{20} respectively) were calculated and used as dosimetric parameters to estimate the effect from the lung volumes irradiated. The restaging FDG PET/CT images were spatially registered to the planning CT using an affine transformation. The transformation was derived from a set of (>1000) matched point pairs generated by an automated point matching algorithm [39] following the approach described by Ourselin et al. [40]. The image registrations were all visually verified for spatial accuracy.

The standard uptake values (SUV) were calculated from the PET attenuation corrected emission images. The mean SUV values in 10-CGE intervals over the dose ranges from 0 to 60 Cobalt-60 Gray equivalents (CGE) in the lung tissue were calculated for each case. The median of SUV mean values and the range of the means for the 100 cases were determined. The maximum SUV value within pulmonary tissue irradiated above 5 CGE was found for all 100 cases. Histograms, normalized by volume, were formed of the FDG PET uptake vs. radiation dose in 2-CGE intervals. SUV values within the lung were normalized to the un-irradiated lung (≤2 CGE) [27]. A linear regression model was applied to the normalized [^{18}F]-FDG uptake for each case to obtain the PMRR. Deviation from the individual linear response was tested for each case.

To test the individual dose response linearity hypothesis multiple models were compared. A purely linear model was compared with models containing the additions of quadratic and logarithm functions of dose into the regression equations. The Akaike Information Criterion (AIC) goodness of fit statistic [41] was used to rate the models. For each model the AIC statistic was calculated as:

$$\mathrm{AIC} = -2 \times \log(\mathrm{MLE}) + 2 \times N_p, \quad (1)$$

where N_p is the number of independent parameters and MLE is the maximized value of the likelihood function for the estimated model. The model minimizing the AIC value provides the best balance between parsimony and goodness of fit. Next, the linear slopes were compared between strictly linear and the combined models.

The medical records were reviewed and scored for respiratory symptoms of pneumonitis using the National Cancer Institute Common Terminology Criteria for Adverse Events, version 4 (CTCAE v4). Briefly, the criteria for CTCAE v4 pneumonitis symptom scoring was: 0 – no signs or symptoms, 1 – diagnostic observations only, 2 – symptoms limiting instrumental activities of daily living (ADLs), 3 – severe symptoms limiting self care or oxygen indicated, 4 – life-threatening respiratory compromise (e.g. intubation), and 5 – death. All patient documents were used in the scoring until 6 months after completing radiation or until esophagectomy. The consensus of six clinicians was used for each score. Clinically symptomatic pneumonitis was defined as grade 2 or higher.

Continuous variables were summarized in the form of mean (SD, range). Categorical variables were summarized in the form of frequency tables. Analysis of variance was used to compare PMRR values across treatment groups. Logistic regression models were used to predict the toxicity outcome (Grade 2 or greater vs. Grade 0–1) according to MLD only,

V20 only, PMRR only, both MLD and V20, both MLD and PMRR, and both V20 and PMRR. Two-fold cross-validation repeated 10,000 times was used to assess the predictive performance of the best model. Statistical analysis was done with SAS version 9 (SAS Institute, Cary, NC) and S-Plus version 7 (Insightful Co., Seattle, WA). Receiver operating characteristic (ROC) curves were generated for each model. The area under the curves (AUC) was determined for each and the corresponding values compared.

Results

The patient characteristics are summarized in Table 1. The prescription dose range was between 45 and 60.6 CGE (median 50.4 CGE) over 28 fractions. The mean lung dose range was 1.0–13.4 CGE (median 5.5 CGE) for all patients. The percent of lung receiving >5 CGE (V_5) was 3.40–59.9% (median 25.4%). The percent receiving >10 CGE (V_{10}) was 2.76–48.7% (median 21.1%). The percent receiving >20 CGE (V_{20}) was 1.18–30.91% (median 10.9%). The interval time from completion of proton radiotherapy until PET/CT imaging was between 21 and 86 days (median 39 days). Patients who received PET/CT less than 20 or greater than 90 days were excluded. There was no significant correlation between the time interval to PET and the resulting mean SUV. The CTCAE v4 scores for pneumonitis were as follows: 36 (36.0%) patients with grade 0; 37 (37.0%) patients with grade 1; 20 (20.0%) patients with grade 2; 7 (7.0%) patients with grade 3. There were no patients (0.0%) with grade 4 or 5 toxicity. Patients who had a toxicity score of 2 or greater were characterized as symptomatic ($n = 27$) and comprised 27% of study subjects. The mean dosimetric parameters for the symptomatic and asymptomatic groups are found in Table 2.

Registered planning CT and PET CT were used to correlate SUV with dose for each patient (Fig. 1). The mean SUV value for the lung receiving between 0 and 10 CGE was 0.64, 10–20 CGE was 0.78, 20–30 CGE was 0.88, 30–40 CGE was 0.94 and 40–50 CGE was 1.02 with an overall median SUV of 0.83. The average SUV uptake for lung treated in symptomatic patients vs. asymptomatic patients was 0.98 and 0.86 respectively ($p = 0.02$). To test the hypothesis of a linear dose response of the lungs to proton radiation for each individual, the additions of quadratic and logarithm functions of dose into the regression equations were tested. We employed the AIC to determine most appropriate model for the FDG uptake dose response from each of the 100 patients, the model with the lowest AIC wins for each case. The winning models were 30 – pure linear, 52 linear quadratic relationship, and 18 linear logarithmic. With the mixed models the linear components were the predominant terms. Comparing the linear coefficients from the linear-quadratic and linear-log models to the linear model slope we found no significant difference using non-parametric tests. The linear dose response slopes from each case (the PMRR values) had a mean of 0.0148 CGE^{-1} (range 0.0002–0.0790 CGE^{-1}).

There was no significant correlation between the PMRR value and the dose received, time interval to PET or the V_5, V_{10} and V_{20}. The generalized linear model revealed that dose is an important predictor of the SUV value. Higher radiation dose corresponds to higher mean SUV values ($p = 0.0001$). The PMRR, MLD, and V_{20} correlated with pulmonary toxicity. The symptomatic group was found to have a higher PMRR. The mean PMRR values of the symptomatic vs. asymptomatic patients were 0.022 and 0.012 respectively ($p = 0.014$) and are shown in Table 2. Fig. 2 shows histogram distributions of the PMRR for the symptomatic and asymptomatic groups. The sensitivity and specificity were estimated from this experiment. Predicted vs. true toxicity for models using MLD, V20, PMRR or combinations of the three are shown in Table 3. The model with the highest area under the ROC curve (AUC ROC) used PMRR and MLD, which had a sensitivity of 45% and specificity of 82%. The AUC for the V_{20} only ROC curve model was 71.0% (95% CI: 59.7–82.3%), for the PMRR only model was 66.1% (95% CI: 54.4–77.7%), for MLD only model

was 72.6% (95% CI: 61.6–83.5%), for the PMRR + MLD model was 73.5% (95% CI: 62.3–84.7%), and for PMRR + V20 model was 73.7% (95% CI: 62.7–84.7%). The model AUC values were not significantly different.

Discussion

This report quantifies the relationship of proton dose and local lung injury. We found a linear relationship between FDG uptake and proton therapy dose predominates for each subject, similar to our prior findings [27]. The slope of the dose response curve (PMRR) varied between patients and its value correlated with the incidence of clinical symptoms. The variation in the individual dose response suggests an underlying difference in the biological response among patients [27,28]. In this study, incorporating the PMRR in models of RP resulted in a slightly larger area under the ROC curve vs. the MLD or V20 alone or their combination, however this increase was not statistically significant.

There are no prospective randomized controlled trials reporting proton therapy for lung cancer [42-44]. Grutters et al. [45] performed a meta-analysis comparing the effectiveness of photons, protons, and carbon ions based on observational studies. They found higher survival rates for particle therapy than for X-ray therapy. Dosimetric comparison studies suggest that proton therapy may reduce radiation pneumonitis risk by reducing the volume of lung irradiated. Chang et al. [46] compared plans between three-dimensional conformal (3D-CRT), intensity-modulated radiotherapy (IMRT), and proton therapy plans for stage I–III lung cancer. Nichols et al. [47] evaluated optimized 3D-CRT, IMRT and proton therapy plans generated for eight consecutive patients with unresectable stage III non-small-cell lung cancer, the proton plans offered a median 31% reduction in MLD. Vogelius et al. [48] compared three alternative treatment plans of 18 non-small cell lung cancer patients previously treated with helical tomotherapy; the tomotherapy plan, an intensity modulated proton therapy plan (IMPT) and a 3D-CRT plan. Proton therapy allowed highly conformal delivery while minimizing the low dose region in the lung. Welsh et al. [49] compared IMRT to intensity-modulated proton therapy in esophagus cancer cases and found IMPT led to considerable reduction in lung dose. In each of these studies, uncertainty exists as to the link between the proton dose distributions and pulmonary toxicity risk [34].

The linear dose response found for proton therapy is similar to that reported for MV X-ray therapy and together they may estimate the proton relative biological effectiveness for RP. The biological effect of proton irradiation (e.g. cell kill) is greater than the effect caused by the same physical dose delivered by X-rays due to the difference in the microscopic distribution of ionizations [50-52]. The ratio of X-ray to proton dose required to achieve the same biological effect is called the relative biological effectiveness (RBE) for proton radiation [53]. RBE values have been measured experimentally *in vitro* with cell lines [54,55] and *in vivo* with rodent models [56,57] by comparing the dose required to achieve the same biological end-points. The PMRR, a surrogate bio-marker for RP, may be utilized as a biological end-point. Consider two matched populations, one who received X-ray and the other proton therapy with population mean PMRR values ($\overline{\text{PMRR}}_{\text{X-ray}}$ and $\overline{\text{PMRR}}_{\text{proton}}$) expressed in identical physical dose units (e.g. Gy^{-1}). Since the dose response is linear for both, the ratio of the X-ray dose necessary to achieve the same FDG PET enhancement as the proton dose is given by the ratio of these slopes and hence the RBE for this endpoint is:

$$\text{RBE}_{\text{RP}} = \frac{\overline{\text{PMRR}}_{\text{proton}}}{\overline{\text{PMRR}}_{\text{X-ray}}}. \quad (2)$$

The incidence of symptomatic RP in this study was within the range (13–37%) reported by Rodrigues et al. [32]. The rate of symptomatic RP was lower in the present study than in our previous retrospective study reported by McCurdy et al. in which the overall incidence of symptomatic radiation pneumonitis was 58% [29]. In that retrospective study, which included 139 patients and one patient who died of fatal radiation pneumonitis, the MLD was 12.3 vs. 7.2 Gy in the present series. This study has several limitations. The time from completion of radiation to restaging PET imaging varied since this is a retrospective study. The time window of restaging PET was chosen based on our previous studies. Pneumonitis was scored using the medical record, however pulmonary comorbidities were not incorporated into the modeling in this study [33]. To improve accuracy of pneumonitis scoring, the consensus of 6 clinicians was used. The PET imaging used in this study were free-breathing, 4D PET may improve quantitative accuracy [58].

In summary, the findings of this study are (1) the pulmonary proton therapy radiation dose response on FDG PET/CT imaging exhibited a predominately linear relationship on statistical modeling and (2) symptomatic patients had a significantly greater dose–response.

Acknowledgments

We extend our warmest gratitude to the thoracic radiation oncologists, thoracic surgeons, and gastrointestinal medical oncologists at M.D. Anderson whose patients comprised this study. This work was partially funded by the National Institutes of Health through a National Cancer Institute Grant R21CA141833 and through an NIH Director's New Innovator Award DP2OD007044. RC was partially supported by an NIH Training Grant T32CA119930.

References

1. Gross NJ. Pulmonary effects of radiation therapy. Ann Intern Med. 1977; 86:81–92. [PubMed: 319723]
2. Bush DA, Dunbar RD, Bonnet R, Slater JD, Cheek GA, Slater JM. Pulmonary injury from proton and conventional radiotherapy as revealed by CT. Am J Roentgenol. 1999; 172:735–9. [PubMed: 10063871]
3. McDonald S, Rubin P, Phillips TL, Marks LB. Injury to the lung from cancer therapy: clinical syndromes, measurable endpoints, and potential scoring systems. Int J Radiat Oncol Biol Phys. 1995; 31:1187–203. [PubMed: 7713782]
4. Van Dyk J, Hill RP. Post-irradiation lung density changes measured by computerized tomography. Int J Radiat Oncol Biol Phys. 1983; 9:847–52. [PubMed: 6345486]
5. Frija J, Ferme C, Baud L, et al. Radiation-induced lung injuries: a survey by computed tomography and pulmonary function tests in 18 cases of Hodgkin's disease. Eur J Radiol. 1988; 8:18–23. [PubMed: 3356195]
6. Sejpal S, Komaki R, Tsao A, et al. Early findings on toxicity of proton beam therapy with concurrent chemotherapy for nonsmall cell lung cancer. Cancer. 2011; 117:3004–13. [PubMed: 21264827]
7. Widesott L, Amichetti M, Schwarz M. Proton therapy in lung cancer: clinical outcomes and technical issues. A systematic review. Radiother Oncol. 2008; 86:154–64. [PubMed: 18241945]
8. Pijls-Johannesma M, Grutters JP, Lambin P, Ruysscher DD. Particle therapy in lung cancer: where do we stand? Cancer Treat Rev. 2008; 34:259–67. [PubMed: 18226466]
9. Nihei K, Ogino T, Ishikura S, Nishimura H. High-dose proton beam therapy for Stage I non-small-cell lung cancer. Int J Radiat Oncol Biol Phys. 2006; 65:107–11. [PubMed: 16458447]
10. Bush DA, Slater JD, Bonnet R, et al. Proton-beam radiotherapy for early-stage lung cancer. Chest. 1999; 116:1313–9. [PubMed: 10559093]
11. Moyers MF, Miller DW, Bush DA, Slater JD. Methodologies and tools for proton beam design for lung tumors. Int J Radiat Oncol Biol Phys. 2001; 49:1429–38. [PubMed: 11286851]

12. Paganetti H, Jiang H, Adams JA, Chen GT, Rietzel E. Monte Carlo simulations with time-dependent geometries to investigate effects of organ motion with high temporal resolution. Int J Radiat Oncol Biol Phys. 2004; 60:942–50. [PubMed: 15465213]
13. Paganetti H, Jiang H, Trofimov A. 4D Monte Carlo simulation of proton beam scanning: modelling of variations in time and space to study the interplay between scanning pattern and time-dependent patient geometry. Phys Med Biol. 2005; 50:983–90. [PubMed: 15798270]
14. Engelsman M, Rietzel E, Kooy HM. Four-dimensional proton treatment planning for lung tumors. Int J Radiat Oncol Biol Phys. 2006; 64:1589–95. [PubMed: 16580508]
15. Engelsman M, Kooy HM. Target volume dose considerations in proton beam treatment planning for lung tumors. Med Phys. 2005; 32:3549–57. [PubMed: 16475753]
16. Kang Y, Zhang X, Chang JY, et al. 4D Proton treatment planning strategy for mobile lung tumors. Int J Radiat Oncol Biol Phys. 2007; 67:906–14. [PubMed: 17293240]
17. Isacsson U, Lennernas B, Grusell E, Jung B, Montelius A, Glimelius B. Comparative treatment planning between proton and X-ray therapy in esophageal cancer. Int J Radiat Oncol Biol Phys. 1998; 41:441–50. [PubMed: 9607363]
18. Zhang X, Zhao KL, Guerrero TM, et al. Four-dimensional computed tomography-based treatment planning for intensity-modulated radiation therapy and proton therapy for distal esophageal cancer. Int J Radiat Oncol Biol Phys. 2008; 72:278–87. [PubMed: 18722278]
19. Koyama S, Tsujii H. Proton beam therapy with high-dose irradiation for superficial and advanced esophageal carcinomas. Clin Cancer Res. 2003; 9:3571–7. [PubMed: 14506143]
20. Sugahara S, Tokuuye K, Okumura T, et al. Clinical results of proton beam therapy for cancer of the esophagus. Int J Radiat Oncol Biol Phys. 2005; 61:76–84. [PubMed: 15629597]
21. Graves PR, Siddiqui F, Anscher MS, Movsas B. Radiation pulmonary toxicity: from mechanisms to management. Semin Radiat Oncol. 2010; 20:201–7. [PubMed: 20685583]
22. Ghafoori P, Marks LB, Vujaskovic Z, Kelsey CR. Radiation-induced lung injury assessment, management, and prevention. Oncology (Huntingt). 2008; 22:37–47. [PubMed: 18251282]
23. Roberts CM, Foulcher E, Zaunders JJ, et al. Radiation pneumonitis: a possible lymphocyte-mediated hypersensitivity reaction. Ann Intern Med. 1993; 118:696–700. [PubMed: 8460855]
24. Fajardo, LF.; Berthrong, M.; Anderson, RE. Radiation pathology. New York: Oxford Univ Press; 2001.
25. Chen DL, Ferkol TW, Mintun MA, Pittman JE, Rosenbluth DB, Schuster DP. Quantifying pulmonary inflammation in cystic fibrosis with positron emission tomography. Am J Respir Crit Care Med. 2006; 173:1363–9. [PubMed: 16543553]
26. Chen DL, Rosenbluth DB, Mintun MA, Schuster DP. FDG-PET imaging of pulmonary inflammation in healthy volunteers after airway instillation of endotoxin. J Appl Physiol. 2006; 100:1602–9. [PubMed: 16424067]
27. Guerrero T, Johnson V, Hart J, et al. Radiation pneumonitis: local dose versus [^{18}F]-fluorodeoxyglucose uptake response in irradiated lung. Int J Radiat Oncol Biol Phys. 2007; 68:1030–5. [PubMed: 17398033]
28. Hart JP, McCurdy MR, Ezhil M, et al. Radiation pneumonitis: correlation of toxicity with pulmonary metabolic radiation response. Int J Radiat Oncol Biol Phys. 2008; 71:967–71. [PubMed: 18495373]
29. McCurdy M, McAleer MF, Wei W, et al. Induction and concurrent taxanes enhance both the pulmonary metabolic radiation response and the radiation pneumonitis response in patients with esophagus cancer. Int J Radiat Oncol Biol Phys. 2010; 76:816–23. [PubMed: 19525073]
30. Moiseenko V, Craig T, Bezjak A, Van Dyk J. Dose-volume analysis of lung complications in the radiation treatment of malignant thymoma: a retrospective review. Radiother Oncol. 2003; 67:265–74. [PubMed: 12865174]
31. Kwa SL, Lebesque JV, Theuws JC, et al. Radiation pneumonitis as a function of mean lung dose: an analysis of pooled data of 540 patients. Int J Radiat Oncol Biol Phys. 1998; 42:1–9. [PubMed: 9747813]
32. Rodrigues G, Lock M, D'Souza D, Yu E, Van Dyk J. Prediction of radiation pneumonitis by dose–volume histogram parameters in lung cancer – a systematic review. Radiother Oncol. 2004; 71:127–38. [PubMed: 15110445]

33. Appelt AL, Vogelius IR. A method to adjust radiation dose–response relationships for clinical risk factors. Radiother Oncol. 2012; 102:352–4. [PubMed: 21981874]
34. Willner J, Jost A, Baier K, Flentje M. A little to a lot or a lot to a little? An analysis of pneumonitis risk from dose–volume histogram parameters of the lung in patients with lung cancer treated with 3-D conformal radiotherapy. Strahlenther Onkol. 2003; 179:548–56. [PubMed: 14509954]
35. Seppenwoolde Y, Lebesque JV, de Jaeger K, et al. Comparing different NTCP models that predict the incidence of radiation pneumonitis. Normal tissue complication probability. Int J Radiat Oncol Biol Phys. 2003; 55:724–35. [PubMed: 12573760]
37. Bruzzi JF, Swisher SG, Truong MT, et al. Detection of interval distant metastases: clinical utility of integrated CT-PET imaging in patients with esophageal carcinoma after neoadjuvant therapy. Cancer. 2007; 109:125–34. [PubMed: 17146785]
39. Castillo E, Castillo R, White B, Rojo J, Guerrero T. Least median of squares filtering of locally optimal point matches for compressible flow image registration. Phys Med Biol. 2012; 57:4827–33. [PubMed: 22797602]
40. Ourselin S, Roche A, Prima S, Avache N. Block matching: a general framework to improve robustness of rigid registration of medical images. Lect Notes Comp Sci. 2000; 1935:557–66.
41. Akaike H. A new look at the statistical model identification. IEEE T Automat Contr. 1974; 19:716–23.
42. Widesott L, Amichetti M, Schwarz M. Proton therapy in lung cancer: clinical outcomes and technical issues. A systematic review. Radiother Oncol. 2008; 86:154–64. [PubMed: 18241945]
43. Goitein M. Trials and tribulations in charged particle radiotherapy. Radiother Oncol. 2010; 95:23–31. [PubMed: 19581014]
44. De Ruysscher D, Mark Lodge M, Jones B, et al. Charged particles in radiotherapy: a 5-year update of a systematic review. Radiother Oncol. 2012; 103:5–7. [PubMed: 22326572]
45. Grutters JPC, Kessels AGH, Pijls-Johannesma M, De Ruysscher D, Joore MA, Lambin P. Comparison of the effectiveness of radiotherapy with photons, protons and carbon-ions for non-small cell lung cancer: a meta-analysis. Radiother Oncol. 2010; 95:32–40. [PubMed: 19733410]
46. Chang JY, Zhang X, Wang X, et al. Significant reduction of normal tissue dose by proton radiotherapy compared with three-dimensional conformal or intensity-modulated radiation therapy in Stage I or Stage III non-small-cell lung cancer. Int J Radiat Oncol Biol Phys. 2006; 65:1087–96. [PubMed: 16682145]
47. Nichols RC, Huh SN, Henderson RH, et al. Proton radiation therapy offers reduced normal lung and bone marrow exposure for patients receiving dose-escalated radiation therapy for unresectable stage iii non-small-cell lung cancer: a dosimetric study. Clin Lung Cancer. 2011; 12:252–7. [PubMed: 21726825]
48. Vogelius IR, Westerly DC, Aznar MC, et al. Estimated radiation pneumonitis risk after photon versus proton therapy alone or combined with chemotherapy for lung cancer. Acta Oncol. 2011; 50:772–6. [PubMed: 21767173]
49. Welsh J, Gomez D, Palmer MB, et al. Intensity-modulated proton therapy further reduces normal tissue exposure during definitive therapy for locally advanced distal esophageal tumors: a dosimetric study. Int J Radiat Oncol Biol Phys. 2011; 81:1336–42. [PubMed: 21470796]
50. Frese MC, Yu VK, Stewart RD, Carlson DJ. A mechanism-based approach to predict the relative biological effectiveness of protons and carbon ions in radiation therapy. Int J Radiat Oncol Biol Phys. 2011; 83:442–50. [PubMed: 22099045]
51. Paganetti H. Interpretation of proton relative biological effectiveness using lesion induction, lesion repair, and cellular dose distribution. Med Phys. 2005; 32:2548–56. [PubMed: 16193785]
52. Paganetti H. Calculation of the spatial variation of relative biological effectiveness in a therapeutic proton field for eye treatment. Phys Med Biol. 1998; 43:2147–57. [PubMed: 9725595]
53. Hall, EJ.; Giaccia, AJ. Radiobiology for the radiologist. Philadelphia: Wolters Kluwer Health/ Lippincott Williams & Wilkins; 2012.
54. Robertson JB, Williams JR, Schmidt RA, Little JB, Flynn DF, Suit HD. Radiobiological studies of a high-energy modulated proton beam utilizing cultured mammalian cells. Cancer. 1975; 35:1664–77. [PubMed: 807318]

55. Matsuura T, Egashira Y, Nishio T, et al. Apparent absence of a proton beam dose rate effect and possible differences in RBE between Bragg peak and plateau. Med Phys. 2010; 37:5376–81. [PubMed: 21089773]

56. Gueulette J, Octave-Prignot Ml, De Coster B-M, Wambersie A, Grégoire V. Intestinal crypt regeneration in mice: a biological system for quality assurance in non-conventional radiation therapy. Radiother Oncol. 2004; 73:S148–54. [PubMed: 15971332]

57. Gueulette J, Blattmann H, Pedroni E, et al. Relative biologic effectiveness determination in mouse intestine for scanning proton beam at Paul Scherrer Institute, Switzerland. Influence of motion. Int J Radiat Oncol Biol Phys. 2005; 62:838–45. [PubMed: 15936568]

58. Aristophanous M, Yong Y, Yap JT, et al. Evaluating FDG uptake changes between pre and post therapy respiratory gated PET scans. Radiother Oncol. 2012; 102:377–82. [PubMed: 22265731]

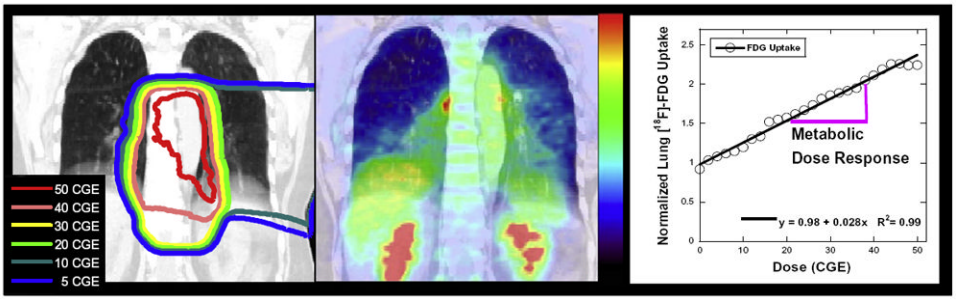

Fig. 1.

Proton dose and FDG PET response in esophagus cancer patients. The proton irradiation isodose distribution delivered to this esophagus cancer patient is shown overlain the treatment planning CT in coronal view in the left panel. The corresponding re-staging [^{18}F]-FDG PET, obtained 6 weeks after completing radiation therapy, is shown overlain the CT in the center panel. There is enhanced FDG activity in the irradiated pulmonary regions. The FDG uptake in lung tissue, normalized to unirradiated lung, vs. the radiation dose (in CGE) is shown in the right panel.

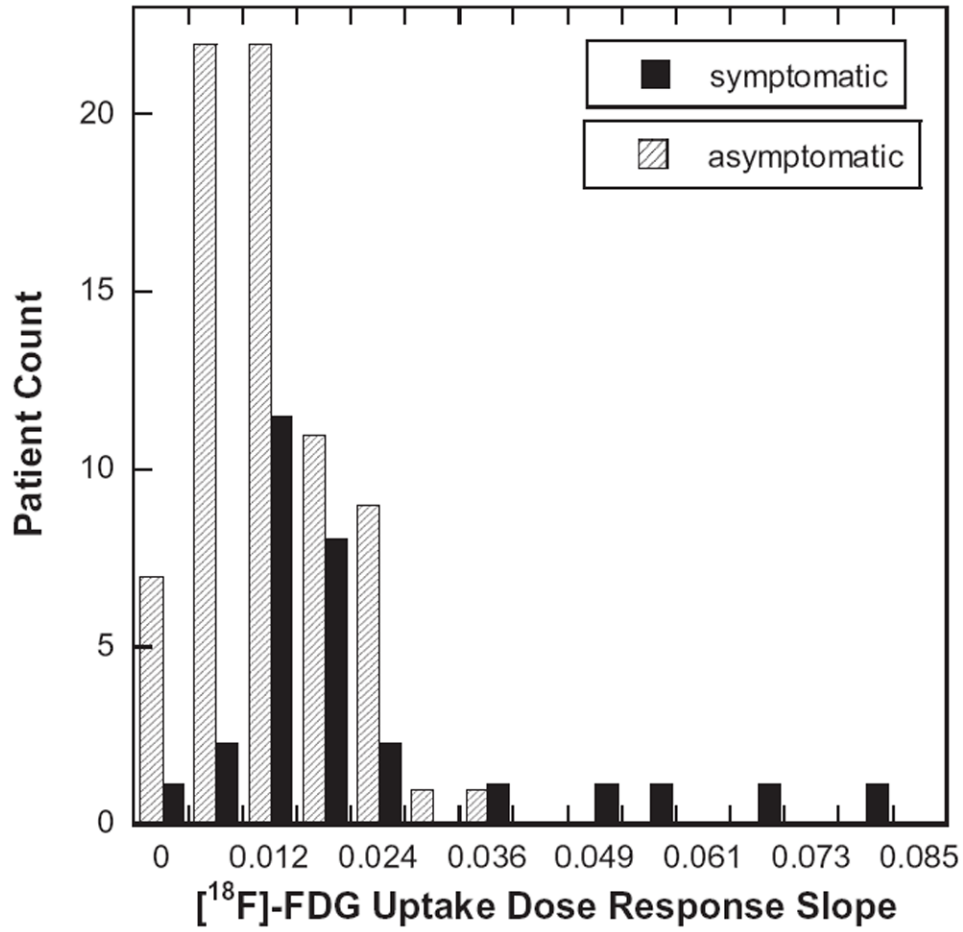

Fig. 2.

Distribution of the pulmonary metabolic radiation dose response (PMRR). A linear regression was applied to the normalized FDG uptake response vs. proton therapy dose for each of the 100 esophagus cancer cases studied in this study. The patients' records were reviewed and scored for symptomatic pneumonitis using CTCAEv4. Symptomatic (CTCAEv4 grade ⩾ 2) and asymptomatic groups were formed and their distributions are shown in histogram plot. The symptomatic group was found to have significantly higher PMRR values ($p = 0.006$).

Table 1

Patient characteristics.

Characteristics	*N* (%)
Age	
Median	66 years
Range	29–83 years
Sex	
Male/female	86/14
Disease stage	
I	3 (3.0)
IIA	24 (24.0)
IIB	6 (6.0)
III	51 (51.0)
IV	7 (7.0)
Recurrent	9 (9.0)
Tumor location	
Proximal	2 (2.0)
Middle	16 (16.0)
Distal/GE junction	82 (82.0)
Prescription dose (CGE)	
Median	50.4
Range	45–60.6
Time between radiotherapy and PET	
Median	39 days
Range	21–86 days
Smoking history	
Yes	80 (80.0)
No	20 (20.0)
Histology	
Adenocarcinoma	83 (83.0)
Squamous cell carcinoma	15 (15.0)
Small cell carcinoma	1 (1.0)
Median follow up time	
Patients undergoing surgery ($n = 67$)	57 days
Patients not undergoing surgery ($n = 34$)	240 days
Concurrent chemotherapy	100 (100)

Abbreviations: GE, gastroesophageal; CGE, Cobalt Gy equivalent.

Table 2

Dosimetric parameters and pulmonary metabolic response rate for symptomatic vs. asymptomatic.

	N	MLD	V5	V10	V20	PMRR	$SUV_{0–10}$	$SUV_{10–20}$	$SUV_{20–30}$	$SUV_{30–40}$	$SUV_{40–50}$
Asymptomatic	73	5.29	23.29	19.37	10.74	0.012	0.65	0.78	0.88	0.97	1.02
Symptomatic	27	7.80	34.89	27.38	15.96	0.022	0.69	0.85	0.98	1.13	1.24
p-value	–	0.0001	<0.0001	<0.0001	<0.0001	0.014	0.797	0.681	0.144	0.115	0.058

All dose values are in CGE = 1.1 × Gy and the PMRR's in CGE^{-1}.

Table 3

Predicted vs. true toxicity for models using MLD, V20, PMRR or combination of the three.

Model	Predicted toxicity status	True toxicity status		Sensitivity (%)	Specificity (%)	PPV (%)	NPV (%)	Accuracy (%)
		Yes	No					
MLD only	Positive	127,257	152,408	47.1	79.1	45.5	80.2	70.5
	Negative	142,743	577,592					
V20 only	Positive	112,577	131,595	41.7	81.9	46.1	79.2	71.1
	Negative	157,423	598,405					
PMRR only	Positive	101,349	156,687	37.5	78.5	39.3	77.3	67.5
	Negative	168,651	573,313					
V20 + MLD	Positive	116,708	152,475	43.2	79.1	43.4	79.0	69.4
	Negative	153,292	577,525					
PMRR + MLD	Positive	121,892	132,102	45.2	81.9	48.0	80.2	72.0
	Negative	148,108	597,898					
PMRR + V20	Positive	118,869	144,713	44.0	80.2	45.1	79.5	70.4
	Negative	151,131	585,287					